

Analytical Study of Electronic Structure in Armchair Graphene Nanoribbons

Huaixiu Zheng,¹ Zhengfei Wang,² Tao Luo,² Qinwei Shi,^{2,*} and Jie Chen^{1,†}

¹*Electrical and Computer Engineering, University of Alberta, AB T6G 2V4, Canada*

²*Hefei National Laboratory for Physical Sciences at Microscale,
University of Science and Technology of China, Hefei, Anhui 230026, People's Republic of China*

We present the analytical solution of the wavefunction and energy dispersion of armchair graphene nanoribbons (GNRs) under the tight-binding approximation. By imposing hard-wall boundary condition, we find that the wave number in the confined direction is discretized. This discrete wavevector serves as the index of different subbands. Our analytical solutions of wavefunction and associated energy dispersion reproduce the results of numerical tight-binding (TB) and the solutions based on the $\mathbf{k} \cdot \mathbf{p}$ approximation. In addition, we also find that all armchair GNRs with edge deformation have energy gaps, which agrees with recently reported first-principles calculations.

PACS numbers:

I. INTRODUCTION

Graphene, as a promising candidate of future nanoelectronic components, has recently attracted intensive research attention.^{1,2,3,4,5,6} Graphene consists of a single atomic layer of graphite, which can also be viewed as a sheet of unrolled carbon nanotube. Several anomalous phenomena ranging from half-integer quantum Hall effect, non-zero Berry's phase³, to minimum conductivity², have been observed in experiments. These unusual transport properties may lead to novel applications in carbon-based nanoelectronics. In addition, the carriers in graphene mimic massless relativistic particles with an effective 'speed of light' $c_* \approx 10^6 m/s$ within the low-energy range ($\epsilon < 0.5 eV$).³ These massless Dirac fermions in graphene allow the test of quantum electrodynamics (QED) phenomena in the low energy range, i.e, Klein paradox.⁶ Ribbons with finite width of graphene, referred to as graphene nanoribbons (GNRs), have also been studied extensively^{7,8,9,10,11,12,13,14}. Recent experimental progress in both the mechanical method^{2,3} and the epitaxial growth method^{4,15} makes possible the preparation of GNRs with various widths.

The carbon atoms on the edge of GNRs have two typical topological shapes, namely armchair and zigzag. The analytical wavefunction and energy dispersion of zigzag nanoribbons have been derived by several research groups.^{16,17} For armchair GNRs, the analytical forms of wavefunctions within the low energy range have been worked out under the effective-mass approximation.¹⁴ It is predicted that all zigzag GNRs are metallic with localized states on the edges^{8,9,16,17}, while armchair GNRs are either metallic or insulating, depending on their widths^{7,8,9,10,14,16}. However, a general expression of the wavefunction of armchair GNRs is still absent until now. In this work, we report the analytical expression of wavefunction and eigen-energy in armchair GNRs. In part II, we first focus on perfect armchair GNRs without any edge deformation and derive the energy dispersion by imposing the hard-wall boundary condition. Due to the quantum confinement, the spectrum breaks into a set of subbands and the wavevector along the confined direc-

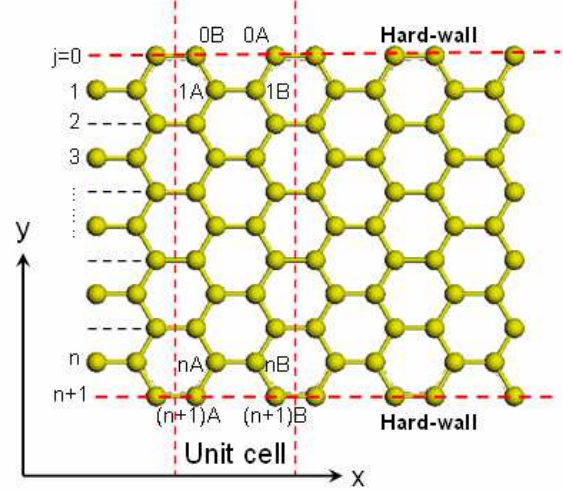


FIG. 1: (color online) Structure of an armchair graphene nanoribbon, consisting of sublattices, A and B. The width of the armchair GNR is n . Every unit cell contains n number of A and B sublattices. Two additional hard walls ($j = 0, n+1$) are imposed on both edges.

tion becomes discretized. We find that the electronic structure of perfect armchair GNRs strongly depends on the width of the ribbon, with the system being metallic when $n = 3m + 2$ and insulating otherwise, where m is an integer.^{7,8,9,10,14,16} Additionally, the low energy electronic structure has been studied. Linear dispersion relation is observed in metallic armchair GNRs. In part III, we evaluate the effect of deformation on the edges. Our calculations show that all armchair GNRs have nonzero energy gaps due to the variation of hopping integral near the edges. This observation is in line with the recently reported first-principles calculated results¹¹.

II. PERFECT ARMCHAIR GRAPHENE NANORIBBON

The structure of armchair GNRs, which consists two types of sublattices A and B, is illustrated in Fig. 1. The unit cell contains n A-type atoms and n B-type atoms. Based on the translational invariance, we choose plane wave basis along the x direction. Within the tight-binding model, the wavefunctions of A and B sublattices can be written as

$$\begin{aligned} |\psi\rangle_A &= \frac{1}{N_A} \sum_{x_{A_i}} \sum_{i=1}^n e^{ik_x x_{A_i}} \phi_A(i) |A_i\rangle \\ |\psi\rangle_B &= \frac{1}{N_B} \sum_{x_{B_i}} \sum_{i=1}^n e^{ik_x x_{B_i}} \phi_B(i) |B_i\rangle, \end{aligned} \quad (1)$$

where $\phi_A(i)$ and $\phi_B(i)$ are the components for A and B sublattices in the y direction, which is perpendicular to the edge. $|A_i\rangle$ and $|B_i\rangle$ are the wave functions of the p_z orbit of a carbon atom located at A and B sublattices, respectively. To solve $\phi_A(i)$ and $\phi_B(i)$, we employ the hard-wall boundary condition

$$\begin{aligned} \phi_A(0) &= \phi_B(0) = 0 \\ \phi_A(n+1) &= \phi_B(n+1) = 0. \end{aligned} \quad (2)$$

Choosing $\phi_A(i) = \phi_B(i) = \sin(\frac{3q_y a}{2}i)$ and substituting them into Eq. (2), we get

$$q_y = \frac{2}{3a} \frac{p\pi}{n+1}, \quad p = 1, 2, \dots, n. \quad (3)$$

q_y is the discretized wave number in the y direction and $a = 1.42\text{\AA}$ is the bond length between carbon atoms. To obtain the normalized coefficients, N_A and N_B , we introduce the normalization condition

$${}_A \langle \psi | \psi \rangle_A = {}_B \langle \psi | \psi \rangle_B = 1.$$

It is straightforward to obtain $N_A = N_B = \sqrt{\frac{N_x(n+1)}{2}}$, where N_x is the number of unit cells along the x direction. The total wavefunction of the system can be constructed by the linear combination of ψ_A and ψ_B

$$\begin{aligned} |\psi\rangle &= C_A \left(\sqrt{\frac{2}{N_x(n+1)}} \sum_{x_{A_i}} \sum_{i=1}^n e^{ik_x x_{A_i}} \sin\left(\frac{3q_y a}{2}i\right) |A_i\rangle \right) \\ &+ C_B \left(\sqrt{\frac{2}{N_x(n+1)}} \sum_{x_{B_i}} \sum_{i=1}^n e^{ik_x x_{B_i}} \sin\left(\frac{3q_y a}{2}i\right) |B_i\rangle \right). \end{aligned} \quad (4)$$

Under tight binding approximation, the Hamiltonian of the system is

$$H = \sum_i \varepsilon_i |i\rangle \langle i| - t_{i,j} \sum_{\langle i,j \rangle} (|i\rangle \langle j|), \quad (5)$$

where $\langle i,j \rangle$ denotes the nearest neighbors.

In perfect armchair GNRs, we set $t_{i,j} = t$ and $\varepsilon_i = \varepsilon$. By Substituting Eq. (4) and Eq. (5) into the Schrodinger equation, we can easily obtain the following matrix expression:

$$\begin{pmatrix} \varepsilon & \mu \\ \mu^* & \varepsilon \end{pmatrix} \begin{pmatrix} C_A \\ C_B \end{pmatrix} = E \begin{pmatrix} C_A \\ C_B \end{pmatrix}, \quad (6)$$

where $\mu = {}_A \langle \psi | H | \psi \rangle_B = t(2e^{ik_x \frac{a}{2}} \cos q_y + e^{-ik_x a})$. Solving Eq. (6), we get the energy dispersion and wavefunction as

$$\begin{aligned} E &= \varepsilon \pm t \sqrt{1 + 4 \cos q_y \cos \frac{3k_x a}{2} + 4 \cos^2 q_y}, \\ |\psi\rangle_{\pm} &= \frac{\sqrt{2}}{2} (|\psi\rangle_A \pm \sqrt{\frac{\mu^*}{\mu}} |\psi\rangle_B). \end{aligned} \quad (7)$$

Here, \pm denotes the conduction and valance bands, respectively. $-\frac{\pi}{2} \leq \frac{3k_x a}{2} \leq \frac{\pi}{2}$ is required within the first Brillouin zone.

Fig. 2 shows the energy dispersion for perfect armchair GNRs with width $n = 6, 7$ and 8 , which reproduce the result obtained by numerical tight-binding method. The electronic structures of armchair GNRs depend strongly on their widths. When $n = 8$, the lowest conduction band and the upmost valence band touches at the Dirac point, which leads to the metallic behavior of $n = 8$ armchair GNRs. Armchair GNRs, however, are insulating when $n = 6$ and $n = 7$. In general, armchair GNRs with the width of $n = 3m+2$ are metallic and insulating otherwise, where m is an integer.^{8,14} In addition, several interesting features appear in the band structures of armchair GNRs.

(i) A flat conduction/valence band exists, if $n=7$. Such a flat band generally corresponds to $\frac{p}{n+1} = \frac{1}{2}$ or equivalently $\cos \frac{p\pi}{n+1} = 0$. The energy dispersion becomes independent of k_x and the eigen-energy always equals $\pm |t|$. It is noticeable that flat band exists only when n is odd.

(ii) The subbands can be labeled by the quantum number p . Combined with the wave number k_x along the x direction, the quantum number p can be used to define the chirality of the electrons in quasi-1D graphene ribbons similar to that in 2D graphene. To identify different subbands, we need the the quantum number p_i of the i th conduction/valence band. Here, the definition of the sequence of subbands is referred to as the value of eigen-energy in the center of first Brillouin zone ($k_x = 0$)

$$E_C = \pm t \left| 2 \cos \frac{p\pi}{n+1} + 1 \right|. \quad (8)$$

For the metallic armchair GNRs with width $n = 3m+2$, when $\frac{p\pi}{n+1} = \frac{2\pi}{3}$ or equivalently $p = 2m+2$, the energy gap between conduction and valence bands is zero. Therefore, $p_1 = 2m+2$ corresponds to the first conduction/valence band in $n = 3m+2$ GNRs. For the second conduction/valence bands, E_C should have the

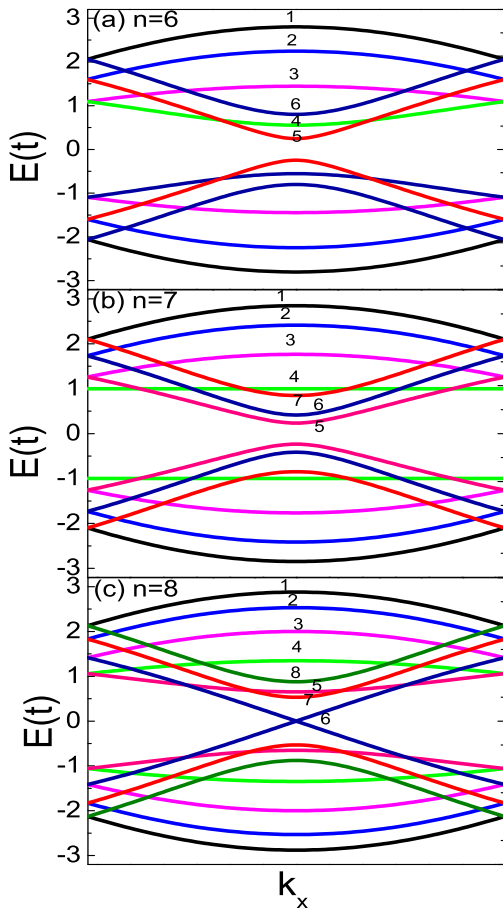


FIG. 2: (color online) Electronic structures of perfect armchair GNRs with width (a) $n=6$ (b) 7 and (c) 8. The wave number is normalized based on the primitive translation vector of individual GNRs. The value of p for each subband is labeled in the figure.

minimal nonzero value compared to the third or even higher band. After analyzing the value of E_C , we find that $p_2 = 2m + 3$, $p_3 = 2m + 1$ for metallic armchair GNRs ($n = 3m + 2$). By similar analysis, for $n > 10$, we can obtain $p_1 = 2m + 1$, $p_2 = 2m$, $p_3 = 2m + 2$ for $n = 3m$ armchair GNRs and $p_1 = 2m + 1$, $p_2 = 2m + 2$, $p_3 = 2m$ for $n = 3m + 1$ armchair GNRs, respectively. For all subbands, there is no general rule of their index.

(iii) The energy dispersion and wavefunction of 2D graphene and 1D GNRs within the low-energy range attract lots of research interest.^{3,11,14} It is well known that low-energy electrons mimic massless relativistic particles in 2D infinite graphene system.^{1,2,3,6,14} Whether electrons keep their relativistic property when

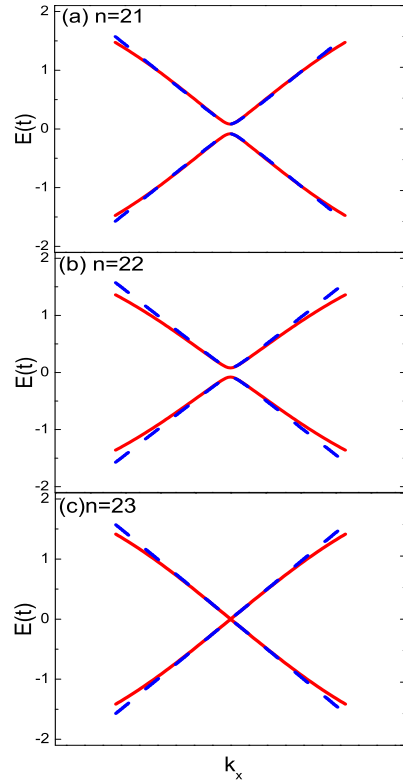


FIG. 3: (color online) The first conductance and valence bands within the first Brillouin zone: exact solutions from Eq. (7) (red solid line) and low-energy approximation from Eq. (10-11) (blue dash line) for armchair GNRs with width (a) $n = 21$ (b) $n = 22$ (c) $n = 23$. The wave number is normalized based on the primitive translation vector of individual GNRs.

they are confined in quasi-1D graphene nanoribbons is an interesting issue. In what follows, we will focus on the expansion of our analytical expressions to the low energy limit. For metallic $n=3m+2$ armchair GNRs, when $\frac{p\pi}{n+1} = \frac{2}{3}\pi$ and $\frac{3k_x a}{2} \rightarrow 0$,

$$E_1(3m+2) = \pm t \sqrt{2 - 2 \cos \frac{3k_x a}{2}} \xrightarrow{k_x \rightarrow 0} \pm \hbar v_F k_x \quad (9)$$

This low energy expansion generates the $E \propto k_x$ linear dispersion, with Fermi velocity $v_F \approx \frac{1}{300}c$. It shows that low-energy electrons in metallic armchair GNRs behave like Dirac Fermions, although they are confined in one direction.

Substituting the value of $p_1 = 2m + 1$ into Eq. (9), we get the low energy expansion of the first conduction/valence band for both $n = 3m$ and $n = 3m + 1$

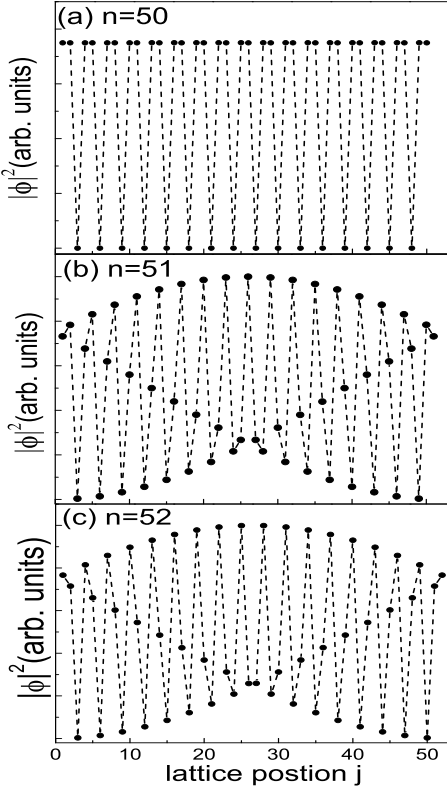


FIG. 4: Local density of the states in the first conduction/valence band at $k_x = 0$ for armchair GNRs with width (a) $n=50$ (b) $n = 51$ and (c) $n = 52$.

armchair GNRs as

$$E_1(3m) \xrightarrow{k_x \rightarrow 0} \pm t \sqrt{\left(\frac{3k_x a}{2}\right)^2 + \left(2 \cos \frac{2m+1}{3m} \pi + 1\right)^2}$$

$$E_1(3m+1) \xrightarrow{k_x \rightarrow 0} \pm t \sqrt{\left(\frac{3k_x a}{2}\right)^2 + \left(2 \cos \frac{2m+1}{3m+1} \pi + 1\right)^2}$$

Fig. 3 shows the quality of low energy approximation. For large width armchair GNRs, low energy approximation seems work well except the edge of first Brillouin Zone. As the width gets larger, the quantum confinement due to the edge becomes less important and the 1D nanoribbons tend to 2D graphene. For large n , as expected, the band structure generates the linear dispersion relationship, $E \propto k_x$ in the low-energy limit.

In addition, from the expression of wavefunction, we also obtain the local density of electronic states in perfect armchair GNRs: $P_A(i) = P_B(i) \propto \sin^2\left(\frac{p\pi}{n+1}i\right)$. Fig. 4 shows the squared wave functions of the lowest conduction band at the center of first Brillouin Zone. Note that Fig. 4(a) and (c) reproduce the results of the $\mathbf{k} \cdot \mathbf{p}$ approximation.¹⁴ The state density oscillates as a func-

tion of the lattice position. The oscillation period is related to $\frac{n+1}{p}$. For $n = 3m + 2$ armchair GNRs, the oscillation period is just 3, which is shown clearly in Fig. 4(a). For $n = 3m, 3m + 1$ armchair GNRs, we should write $\frac{n+1}{p}$ into irreducible form $\frac{i}{j}$. The oscillation period is then i . For $n = 51$ and $n = 52$, we get $i = 51$ and $i = 52$ respectively. As shown in Fig. 4(b) and (c), the oscillation period of state density for $n = 51$ and $n = 52$ armchair GNRs equals their width.

III. EDGE DEFORMATION AND ENERGY GAP

Because every atom on the edge has one dangling bond unsaturated, the characteristics of the $C - C$ bonds at the edges can change dramatically.^{10,19} To determine the band gaps of GNRs on the scale of nanometer, edge effects should be considered carefully since the change of edge bonds length and angle can lead to considerable variations of electronic structure, especially within the low energy range.^{11,12} In previous work, the edge carbon atoms of GNRs are all passivated by hydrogen atoms or other kinds of atoms/molecules.^{10,11,12,14,19} The bonds between hydrogen and carbon are differ from those $C - C$ bonds. Accordingly, the transfer integer of the $C - H$ bonds and on-site energy of carbon atoms at the edges are expected to different from those in the middle of GNRs. The bond lengths between carbon atoms at the edges are also predicted to vary about 3% – 4% when hydrogenerated.¹¹ Correspondingly, the hopping integral increases about 12% extracted from the analytical TB expression.^{11,18} To evaluate the effect of various kinds of edge deformation, we carried out general theoretical calculation and analysis with our analytical solution of armchair GNRs. Generally, we set the variation of the transfer integer and on-site energy as $\delta t_{i,j}, \varepsilon_i$ for the i th A-type and B-type carbon atoms in the unit cell. The Hamiltonian of the GNRs with deformation on the edge can be rewritten as

$$H = \varepsilon_i \sum_i |i\rangle \langle i| - \sum_{\langle i,j \rangle} (t + \delta t_{i,j}) |i\rangle \langle j| \quad (10)$$

It is readily to obtain the energy dispersion and wavefunction by solving the Schrodinger equation

$$E = \gamma \pm |\mu + \delta\mu|$$

$$|\psi\rangle_{\pm} = \frac{\sqrt{2}}{2} (|\psi\rangle_A \pm \sqrt{\frac{(\mu + \delta\mu)^*}{\mu + \delta\mu}} |\psi\rangle_B), \quad (11)$$

where $\gamma = \frac{2}{n+1} \sum_{i=1}^n \varepsilon_i \sin^2\left(\frac{p\pi}{n+1}i\right)$ is the energy shift originating from the variation of on-site energy, while the

energy shift from the hopping integral variation is

$$\begin{aligned} \delta\mu = & -\frac{2t}{n+1} \sum_{i=1}^n [\delta t_{i(A)i(B)} \sin^2\left(\frac{p\pi}{n+1}i\right) e^{-ik_x a} \\ & + \delta t_{i(A)i-1(B)} \sin\left(\frac{p\pi}{n+1}i\right) \sin\left(\frac{p\pi}{n+1}(i-1)\right) e^{\frac{ik_x a}{2}} \\ & + \delta t_{i(A)i+1(B)} \sin\left(\frac{p\pi}{n+1}i\right) \sin\left(\frac{p\pi}{n+1}(i+1)\right) e^{\frac{ik_x a}{2}}]. \end{aligned} \quad (12)$$

Such a general expression could include various kinds of edge deformations, ranging from the quantum confinement effect due to the finite width, to the effect of saturated atoms or molecules attached to edge carbon atoms. In general, this result shows that the deformation leads to a considerable deviation of the energy dispersion relation and wavefunction of the deformed system from those in perfect armchair GNRs. The local state density on both kinds of sublattices, however, remains the same as that in perfect armchair GNRs. The reason is that the wavefunctions of sublattices A and B change their relative phases, but keep the magnitudes unchanged. The variations from both the on-site energy and hopping integral contribute to the energy shift, while, the change of on-site energy has no contribution to the wavefunction as shown in Eq. (8). To verify our findings, we reproduce the energy gap observed in Son's recent work¹¹ by considering only the variation of hopping integrals of the bonds on the edges ($\delta t_{11} = \delta t_{nn} = \delta t$, others equal to zero.). The corresponding energy gaps for different width ribbons are as follows:

$$\begin{aligned} \Delta_{3m} &= \Delta_{3m}^0 - \frac{8\delta t}{3m+1} \sin^2 \frac{m\pi}{3m+1}, \\ \Delta_{3m+1} &= \Delta_{3m+1}^0 + \frac{8\delta t}{3m+2} \sin^2 \frac{(m+1)\pi}{3m+2}, \\ \Delta_{3m+2} &= \Delta_{3m+2}^0 + \frac{2\delta t}{m+1}, \end{aligned} \quad (13)$$

where Δ_{3m} , Δ_{3m+1} and Δ_{3m+2} are the energy gaps of perfect armchair GNRs. Their values can be extracted

from Eq.(8): $2t \left| 2 \cos \frac{(2m+1)\pi}{3m+1} + 1 \right|$, $2t \left| 2 \cos \frac{(2m+1)\pi}{3m+2} + 1 \right|$ and 0. This result suggests all armchair graphene ribbons with edge deformation have nonzero energy gaps and are insulating correspondingly.

IV. CONCLUSION

In this paper we study the electronic states of armchair GNRs analytically. By imposing the hard-wall boundary condition, we derive the analytical solution of the wavefunction and energy dispersion in armchair GNRs with tight-binding approximation. Our results can reproduce the numerical tight-binding calculation solutions based on the effective-mass approximation. We also find the low-energy approximation of the energy dispersion, which matches the exact solution at the edge of first Brillouin zone. The linear energy dispersion is observed in metallic armchair GNRs with the low energy limit. This result suggests that electrons in metallic armchair GNRs behave like Dirac Fermions. Lastly, we evaluate the effect of the edge deformation and give a general expression of wavefunction and energy. We reproduce the energy gap for hydrogenerated armchair GNRs presented in Ref.¹¹. Overall, our proposed analytical wavefunction form provide a powerful analytical tool for quantitatively investigating and predicting various properties in armchair graphene ribbons.

ACKNOWLEDGMENT

This work is partially supported by the National Natural Science Foundation of China, by National Key Basic Research Program under Grant No. 2006CB0L1200, by the USTC-HP HPC project, and by the SCCAS and Shanghai Supercomputer Center. Jie Chen would like to acknowledge the funding support from the Discovery program of Natural Sciences and Engineering Research Council of Canada (No. 245680). We also would like to thank Nathanael Wu and Stephen Thornhill for their assistance with the finalization of this paper.

* Corresponding author. E-mail: phsqw@ustc.edu.cn

† Corresponding author. E-mail: jchen@ece.ualberta.ca

¹ K. S. Novoselov, A. K. Geim, S. V. Morozov, D. Jiang, Y. Zhang, S. V. Dubonos, I. V. Grigorieva, and A. A. Firsov, *Science* **306**, 666 (2004).

² K. S. Novoselov, A. K. Geim, S. V. Morozov, D. Jiang, M. I. Katsnelson, I. V. Grigorieva, S. V. Dubonos and A. A. Firsov, *Nature* **438**, 197 (2005).

³ Yuambo Zhang, Yan-Wen Tan, Horst L. Stormer1, and Philip Kim, *Nature* **438**, 201 (2005).

⁴ Claire Berger, Zhimin Song, Xuebin Li, Xiaosong Wu, Nate Brown, Cécile Naud, Didier Mayou, Tianbo Li, Joanna

Hass, Alexei N. Marchenkov, Edward H. Conrad, Phillip N. First and Walt A. de Heer, *Science* **312**, 1191 (2006).

⁵ Taisuke Ohta, Aaron Bostwick, Thomas Seyller, Karsten Horn and Eli Rotenberg, *Science* **313**, 951 (2006).

⁶ M. I. Katsnelson, K. S. Novoselov, A. K. Geim, *Nature* **2**, 620 (2006).

⁷ M. Fujita, K. Wakabayashi, K. Nakada, K. Kusakabe, *J. Phys. Soc. Jpn* **65**, 1920 (1996).

⁸ K. Nakada, M. Fujita, G. Dresselhaus, M. S. Dresselhaus, *Phys. Rev. B* **54**, 17954 (1996).

⁹ K. Wakabayashi, M. Fujita, H. Ajiki, M. Sigrist, *Phys. Rev. B* **59**, 8271 (1999).

¹⁰ M. Ezawa, Phys. Rev. B (73), 045432 (2006).

¹¹ Y.-W. Son, M. L. Cohen and S. G. Lioue, Phys. Rev. Lett. (97), 216803 (2006).

¹² Y.-W. Son, M. L. Cohen and S. G. Lioue, Nature (London)(444), 347 (2006).

¹³ Y. Miyamoto, K. Nakada, M. Fujita, Phys. Rev. B **59**, 9858 (1999).

¹⁴ L. Brey and H. A. Fertig, Phys. Rev. B (73), 235411 (2006).

¹⁵ C. Berger et al., J. Phys. Chem. B (108), 19912 (2004).

¹⁶ Ken-ichi SASAKI, Shuichi MURAKAMI and Riichiro SAITO, J. Phys. Soc. Jpn. **75** (2006) 074713.

¹⁷ K. Sasaki, S. Murakami and R. Saito, Appl. Phys. Lett. (88), 113110 (2006).

¹⁸ D. Porezag et al., Phys. Rev. B (51), 12947 (1995).

¹⁹ T. Kawai, Y. Miyamoto, O. Sugino, and Y. Koga, Phys. Rev. B (62), R16349 (2000).